Chapter 11

Investigation of Ring Waveguide Add/Drop with Grating Couple

Jian-Chiun Liou

Additional information is available at the end of the chapter

http://dx.doi.org/10.5772/intechopen.76800

Abstract

The silicon photon technology platform is low transmission loss, small size, low cost of the process and easy integration with electronic components and other characteristics. It is designed to design high-density optical communication network system has a considerable advantage. Such as high-density wavelength division multiplexing (DWDM) system, that is through the different wavelengths of signal processing. So that it can be used for optical connection switches, routing and other applications. It composed of a DWDM system, through the Mach-Zehnder interferometer, ring resonator (Add/Drop), array waveguide grating (AWG) and grating coupler and other structural components. It is designed by components to filter, switch, adjust and detect functions. The characteristics of the ring resonator are for wavelength selection. It is suitable for the design of optical switches, signal switching and modulation applications. It is also the focus of this lab and this chapter to explore and study. The general edge coupling, between the optical fiber and the waveguide dimension is very different. As a result, larger insertion loss is caused. This study uses the vertical coupling method to investigate the characteristics of a ring resonator.

Keywords: ring waveguide, add/drop, grating couple

1. Introduction

Big data era is entering reality. However, due to the limitations of electronic physical characteristics, the traditional electrical interconnect [1–12] are increasingly faced with the challenge of rapidly expanding data transmission due to their technical development. In terms of bandwidth expansion, transmission delay, loss control, signal enhancement and other aspects of the urgent need for a fundamental breakthrough. This prompted researchers to start looking

for new solutions. Si-based photonic devices use optical transmission signals. Compared to electrons, photons travel much faster than the electron's velocity, and the mechanism by which light transmits signals is the wave impedance transformation, which consumes very little energy. The signal is not prone to distortion during transmission. In large bandwidth conditions can be greater transmission capacity. And silicon-based photonic devices also have complementary metal oxide semiconductor (CMOS) process compatible, small size, communication band transparent, anti-radiation and so on. It is precisely because of large bandwidth, low latency, low power consumption, low crosstalk and other advantages [13–21]. Emerging information technologies such as optical communications, optical interconnects and optical sensing based on the integration of silicon photonics demonstrate the development trend of building new information hardware. It is becoming an important foundation for a new generation of information systems and networks. A key issue that cannot be ignored for Si-based photonic integrated chips is the input and output of optical signals. In particular, silicon is an indirect bandgap material. Luminous efficiency has not yet reached the practical requirements. The prior art approach required the introduction of a separate light source from outside the photonic chip or the use of an on-chip hybrid integrated light gain material. Therefore, the photonic integrated chip needs among high efficiency, large bandwidth and easy integration of the optical coupling structure both in and out of the chip. Commonly used two kinds of coupling methods generally use the end level coupling structure or on-chip vertical coupling structure. It is compared to other various opto-couplers. The grating coupler uses the vertical diffractive optical field of the on-chip optical waveguide to realize the optical signal input or output of the wafer. It has the advantages of easy online on-chip testing, no wafer or wafer pretreatment, and no strict space limitations. Become a hot spot in the field of silicon-based photonics integration. With the gradual improvement of CMOS process accuracy. Silicon-based waveguides at or near the nanometer level are gradually getting out of the process limitations [22–36]. Raster coupler also gradually shows its unique technical advantages. This research mainly expounds the development status and future trend of grating coupler in recent years.

2. Grating coupler and characteristics

Silicon-based grating coupled devices can be divided into one-dimensional structure and two-dimensional structure. According to the grating cell cycle, duty cycle, etching depth, etching angle can be divided into uniform grating coupler, non-uniform grating coupler and blazed grating coupler. Gratings are coupling functional devices in silicon-based photonic integrated wafers. The main research contents of grating coupler include coupling efficiency, coupling angle, working wavelength bandwidth, polarization correlation and so on.

This uniform grating coupler refers to the unit period of each grating as shown in **Figure 1**, duty cycle, etching depth are constant. Its structure is that the slit is generally perpendicular to the interface. The diffraction mode field of a uniform periodic grating coupler decays exponentially. The mode field of single mode fiber is Gaussian distribution. The overlap between the two η_3 is limited. This is a classic model of a grating coupler. The coupling efficiency of the grating coupler is a coupling efficiency η_3 determined by the diffraction intensity, the

http://dx.doi.org/10.5772/intechopen.76800

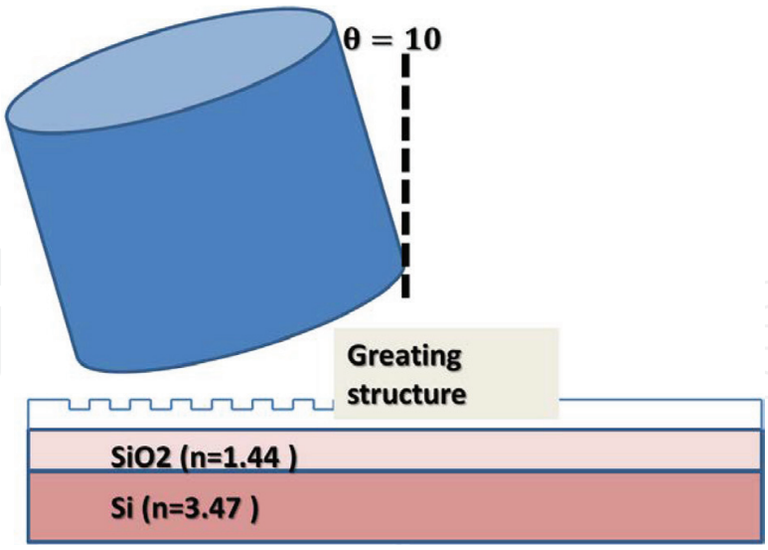

Figure 1. Silicon-based grating coupled.

directional efficiency and the overlapping integral of the coupling light field. Coupling efficiency is greatly affected. It is difficult to achieve efficient coupling. There are many ways to enhance the coupling efficiency. For example, an increase of multilayer dielectric mirrors, metal mirrors, overlays, and large duty cycle grating structures utilizing the slot effect. These methods either reduce reflection or enhance directivity, or reduce the reflection loss between the grating coupler and the optical fiber. This attenuated diffraction mode field and the optical mode field overlap integral is small. Coupling efficiency is greatly limited. The advantage of a uniform grating coupler is CMOS-compatible. The process is relatively simple. Moreover, the study of uniform structure is more comprehensive. Its processing method is more mature.

Non-uniform grating coupler effectively solves this mode field mismatch problem. The so-called non-uniform grating coupler, refers to the cycle and duty cycle or etching depth changes with the direction of light a quasi-periodic structure. Due to the fact that this structure no longer maintains a strict periodicity, the diffraction factor changes correspondingly as the grating cell structure changes. Therefore, the diffraction mode field no longer exhibits its exponential decay. It is theoretically possible to achieve a Gaussian distribution of the diffracted light field. A non-uniform grating coupler structure exhibiting a Gaussian type in the diffraction mode field can be formed by a set of narrow-width-expanded slits. Etch depth from shallow to deep. This waveguide-to-grating reduction of the structure reduces the reflection loss, which is very helpful in improving the coupling efficiency due to the process challenges. This grating coupler structure developed slowly from the theory. One commonly used method of controlling the depth of etching is to take advantage of the load (hysteresis) effect of plasma etching. Optimize the correspondence between etching depth and slit width.

This is with the improvement of craftsmanship. Fine structures below 50 nm are also possible. The minimum width of the non-uniform grating coupler made by our research group is about 40 nm. The experimentally measured single-ended coupling loss is only 0.85 dB. Solve the problem of non-uniform periodic grating coupler on the fine processing requirements.

Researchers at OFC/NFOEC 2013 presented a method for double-depth etching, as shown in **Figure 3(a)** . This method uses several pairs of shallow etched raster to replace the front narrow groove grating pairs. This is due to the shallow depth of etching. It reaches the same coupling strength as the deep etched grating. It is necessary to increase the width of the groove. Reduce the technical difficulty. The minimum groove width in this article is 135 nm. The coupling loss is about 1.5 dB in the vertical coupling structure.

All along, to enhance the technology is to reduce the second-order reflections. It is improving the coupling efficiency. The grating coupler diffraction angle is about 10° angle. But this kind of declination not only has the limitation to the practical application. It caused packaging difficulties. Hinder the large-scale integration of the device. Vertical coupling becomes another problem to be solved that limits the practical application of the grating coupler after the coupling efficiency. For 0° declination, which is the need for vertical coupling is even more pressing. It is a uniform grating coupler or a non-uniform grating coupler. The problem of vertical coupling has not been well solved. There is second order reflection in resonance state. Second order reflection greatly reduces the coupling efficiency. In the detuning state, the second order reflections disappear. Coupling efficiency increases, but vertical coupling cannot be achieved. It can be seen from the Prague relations that it is to achieve vertical coupling. It must eliminate or reduce the second order reflections. Known methods have been the addition of distributed Bragg reflector (DBR) mirrors. The reflected light of the DBR mirror is canceled by the interference of the second order reflected light.

In this study, vertical coupling of 40% coupling efficiency was achieved by adding DBR mirrors. Its efficiency is close to the coupling efficiency (44%) without a DBR mirror. It is only weakening second-order reflections by process deviation. It cannot be completely eliminated. Coupling efficiency curve will fluctuate. And DBR reflector parameters of the process control are difficult. Changing the distance between the coupler and the mirror by 100 nm cancels out the interference and constructs the interference phase. The efficient is coupling into a great loss. Therefore, it is necessary to further study and improves the DBR mirror grating structure is the best way to eliminate second-order reflection is blazed grating. The slits of the blazed grating are not perpendicular to the wafer surface. Instead, there is a blaze angle in the normal direction of the raster plane. The diffraction mode field is the superposition of the total diffraction mode field. Blazed grating processing requirements is incompatible with CMOS process. For the process of the problem, the research proposed a gradual change of the gradient grating coupler. Use the multi-step structure instead of the inclined surface of the blazed grating. Asymmetric sub-grating structures proposed by researchers can theoretically be vertically coupled. At the same time coupling efficiency is not much loss.

3. Two-dimensional grating coupler

Two-dimensional grating coupler can be roughly divided into two kinds. One is a grating coupler similar to a photonic crystal structure. The other is the curved grating coupler. The two-dimensional photonic crystal grating coupler is proposed to solve the polarization problem in the grating waveguide as shown in **Figure 2**. The large difference is in the transmission

http://dx.doi.org/10.5772/intechopen.76800

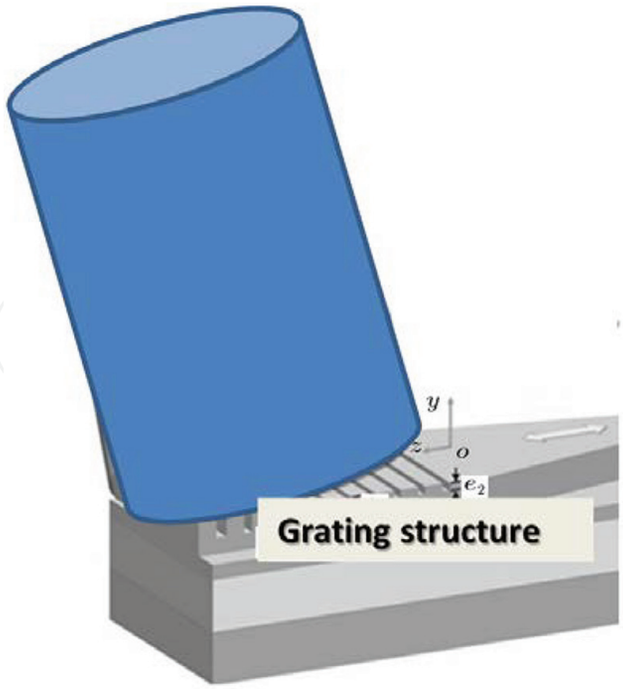

Figure 2. Two-dimensional grating coupler.

characteristics of the two transmission modes (TE, TM mode) in the grating coupler. A typical grating coupler can only transmit one mode. Transmission loss to another mode is relatively large. Waveguide birefringence is commonly used to describe polarization dependence. Defined as the difference between the effective refractive index or the group refractive index of the TE and TM modes, $\Delta n = nTE_{eff} - nTM_{eff}$. TE_{eff} and TM_{eff} are refractive index of the TE and TM modes. The ideal polarization correlation is zero. Zero birefringence is the inability to precisely control the waveguide size. Smaller size deviations result in changes in polarization dependence. In addition, the polarization dependence is also related to the heat outside the waveguide, pressure, etc., to achieve polarization insensitivity is very difficult.

A grating coupler for a two-dimensional photonic crystal is another solution. The light of different polarization state is separated in the grating coupler. In one path, the TM mode is changed into the TE mode, and the TE mode is transmitted in different waveguides. Finally, it received by another two-dimensional photonic crystal grating coupler. Compared with the former method, the process is relatively less difficult. This grating coupler requires exactly two waveguide devices. Otherwise there will be distortion in the synthesis. Arc grating coupler can effectively increase the degree of integration. Grating couplers and transmission waveguides typically have a pitch of more than 100 μm. An arcuate grating coupler takes advantage of the optical focusing characteristics of a circular or oval structure. All the arcs have a common focus. The waveguide is placed at this focus. This greatly reduces the spacing between the grating region and the waveguide. Arc grating coupler and waveguide spacing is generally 20 μm or less. Arc grating coupler increases the integration density at the same time. The additional loss between the waveguide and the waveguide is also reduced. The reported coupling efficiency of the curved grating coupler is 1.25 dB.

An infinitely long uniform grating with wavelength selectivity, in practical applications, the grating length is limited. This creates a spectral broadening. This broadening has a certain limit. Since the grating structure parameters of the non-uniform grating coupler are not fixed values. According to the Bragg formula, the diffracted waves no longer maintain a single wavelength. Chirp Structure in Non-uniform Grating Coupler. It is raised in order to improve the bandwidth. It compared to a uniform grating coupler. Chirped grating adds a concept of chirp. It is usually the grating cell cycle changes. The increase in bandwidth is mainly determined by the amount of chirp. The University of Hong Kong used a "fishbone" structure in the fabrication of sub-wavelength waveguide grating coupling devices. Compared to normal grating structures, this fishbone The 3 dB bandwidth of the structured grating coupler increases while reducing the back reflection, reaching 90 around 1530 nm, while the curved grating reduces the transmission loss with a theoretical result of 1.7 dB The grating coupling loss is 3.5 dB.

The chirped grating used in this study is a chirp structure with uniformly varying periods. The grating period changes linearly. Analogies show that the 3 dB bandwidth of a chirped grating increases to 140 nm at a grating average period of 700 nm, a chirp of 200 nm and a grating period of 20. The center wavelength is in the vicinity of 1550 nm. The experimentally measured 3 dB bandwidth is 120 nm, which is similar to the simulation results.

4. Ring waveguide add/drop

3D drawing of ring laterally coupled (left) and vertically coupled (right) to the straight waveguides.

The general application of this silicon-on-silicon micro-ring thermocouple switch is shown in **Figure 3**. The advantages of silicon nanocrystals are absorbing layers instead of polymer materials. It is compatible with standard micro-process technology. Silicone crystals have a wide absorption band which can extend close to the IR band. This system includes several features, the temperature dependence of refractive index. Silicon materials usually have higher refractive index temperature dependence than glass materials. Silicon temperature coefficient of about −0.075/°C grade. It is suitable for thermo-optic switch, silicon material refractive index temperature dependence. Other inorganic material temperature difference is relatively large and unstable. Silicon materials have low voltage, low current drive characteristics. It is switching time up to a few msec. It is suitable for wavelength tunable filter. It is heated silicon material refractive index increases. The wavelength of the optical filter will move towards long wavelengths. When the pulse wave is added, the rise time is about 25 msec and the fall time is about 30 msec. Waveform is high on (Pump on) 150 msec. The resulting power is 3.4 μW, low off (Pump off) 150 msec. It corresponds to the thermal optical switch displacement resonance wavelength of about 5 pm. Grating coupling effects via micro-cycle. This design structure is the most original resonant spectrum output to the optical detector. It observes resonance waves. It supplies a pulse of power to make the resonance wave read out by the optical detector displacement spectrum.

http://dx.doi.org/10.5772/intechopen.76800

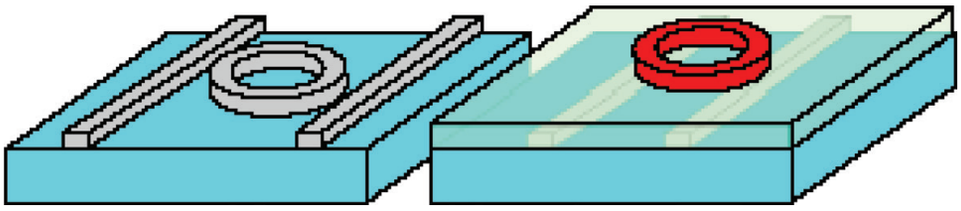

Figure 3. 3D drawing of ring laterally coupled (left) and vertically coupled (right) to the straight waveguides.

The thermo-optic switch calculates the switching energy, $H = hA\delta T$, where h is the total switching energy of the resonant center wavelength to be shifted, which is calculated by dividing the energy of the silicon (~ 10^{-5}/° C). The material heat transfer coefficient in the air, A is the sphere size. This circle diameter is 150 μm, Q = 3 × 10^{-5} its resonance wavelength at 1450 nm, so the wavelength shift is ~ 4.8 pm. = 4.8/10 = 0.48° C, h = 81 W/m²/° C for silicon rings. It calculate the required switching energy H = 2.9 μW.

The microsphere temperature reaches equilibrium after power is turned on and off. In other words, that in these microspheres must reach a certain temperature stable in the surrounding air. in order to make the desired resonant frequency shift very accurately fall in the desired band. The pulse signal has a very good control of the drive. This study based on micro-ring heat. The optical switch specially designs the precise power signal control circuit, which obtains better optical information processing efficiency for further breakthrough in the optical communication field.

5. Experiment and results

Edge coupler for wavelength selection platform is shown in **Figure 4**. The characteristics of a micro-switch ring wavelength selective switch are analyzed. The working states of the components and corresponding switching operations are analyzed. A new light intensity transfer function formula is used to numerically compare the spectral responses of different operating states and the switching responses of different switching operations. The results show that the device can realize the signal wavelength of four ways of simultaneous access of three channels, simultaneous access of two channels, single-channel access and no-channel access Selective access, multi-channel access to the open-circuit crosstalk performance deterioration, off-state crosstalk performance is not affected. The realization of the device access conversion between the switching operation can be divided into three categories. It switches operation to achieve the best off. The change of the index of refraction of small micro-rings during state crosstalk is about 6.0 × 10^{-3}. The value of the change refraction index is in small micro-rings. It fully switched is less than 8.0 × 10^{-4}. It indicates that it is easy to realize by thermo-optic effect Switching operation, and temperature control of the larger tolerance, the loss of the device switching characteristics of the results show that the loss can be based on the actual value. The refractive index of the micro-ring value of the passage is closed.

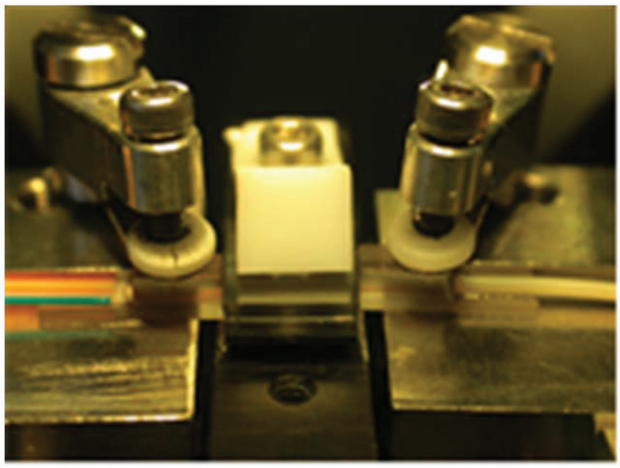

Figure 4. Edge coupler for wavelength selection platform.

In photonic multiplexing signal processing circuit, it can change the frequency and output amplitude of the size of the functional circuitry. Multiprocessing signal function lies in the large optical switch array selection (Addressing). It can quickly indicate which one of the optical switches is going to act as a thermo-optic effect as shown in **Figure 5**. It is fed into the desired temperature relative to the waveform and amplitude selected. It causes the temperature to be generated to correspond to this wavelength (λ). This so-called exchange of light signals is controlled by the thin film heating elements distributed in the polymer stack. The current through the heater cause the metal film heat as shown in **Figure 6**. It changes the distribution of heat within the branching area of the waveguide, causing the refractive index of the waveguide below it to change. It can guide the optical coupling from the main waveguide to the target branch waveguide, and realize the light switching action as shown in **Figure 7**.

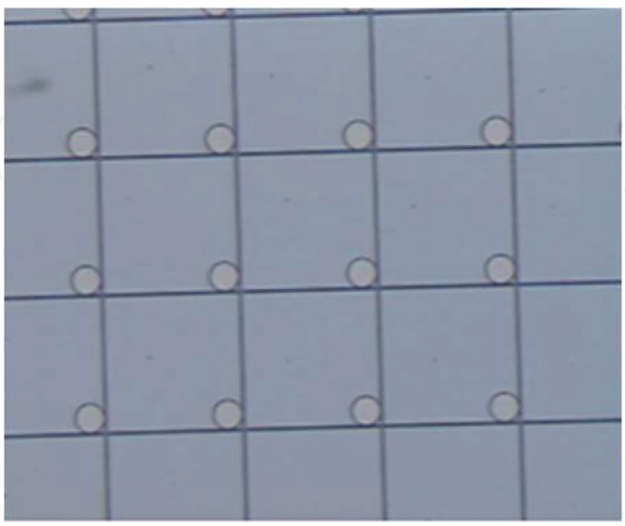

Figure 5. The optical micro-ring switches.

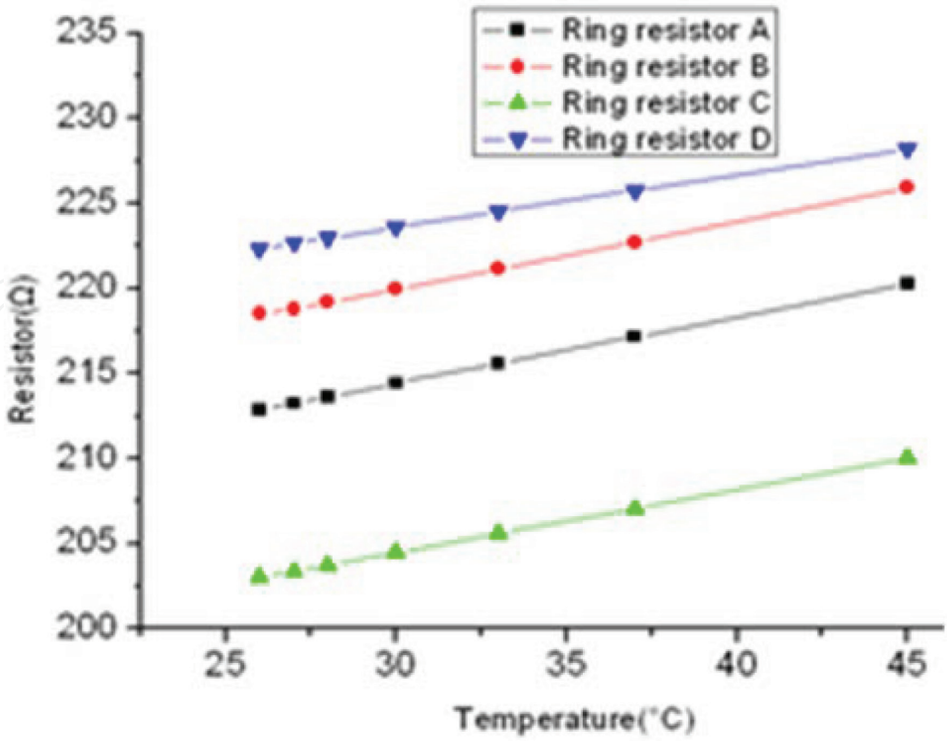

Figure 6. Different ring resister with difference value of temperature.

The system delivers laser light through a tunable laser (Yenista Tunicss-T100S) with a wavelength range of 1490 to 1640 nm and a resolution of 1 pico-meter. The laser light is transmitted through the fiber to a 2 × 2 splitter The splitter transmits the laser light to one end of the Gas cell and one end of the polarization controller respectively. Gas cell can generate absolute position at a specific wavelength. It is able to generate wavelength calibration position axis for the measurement of components. Through the polarization controller is the component side. It is through the polarization controller to control the maximum intensity of light detector straight. Laser light is TE polarized incident. It propagates through the fiber and is coupled through two grating couplers. At the same time through both ends of the InGaAs photodetector with amplification function to receive the last as shown in **Figure 8**. The system converts the measured optical signal into an electrical signal. It is through the BNC cable to send data to the computer.

In Add/drop condition is shown in **Figure 9**, an incident light enters from the input port of the optical waveguide. Part of the energy continues to propagate forward through the coupling region during transmission. A portion of the energy is coupled to the ring resonator. The energy coupled to the ring resonator is after a half-turn. A portion of the energy is coupled to the drop port. After the remaining energy is further circulated for half a turn, a part of the energy will be coupled back to the optical waveguide. The remaining energy will continue to maintain the above mechanism for dissemination. It is until the energy depleted so far. It is selectivity to wavelengths through the ring resonator. It can effectively filter or capture the wavelength of the action. It can achieve the effect of controlling the wavelength.

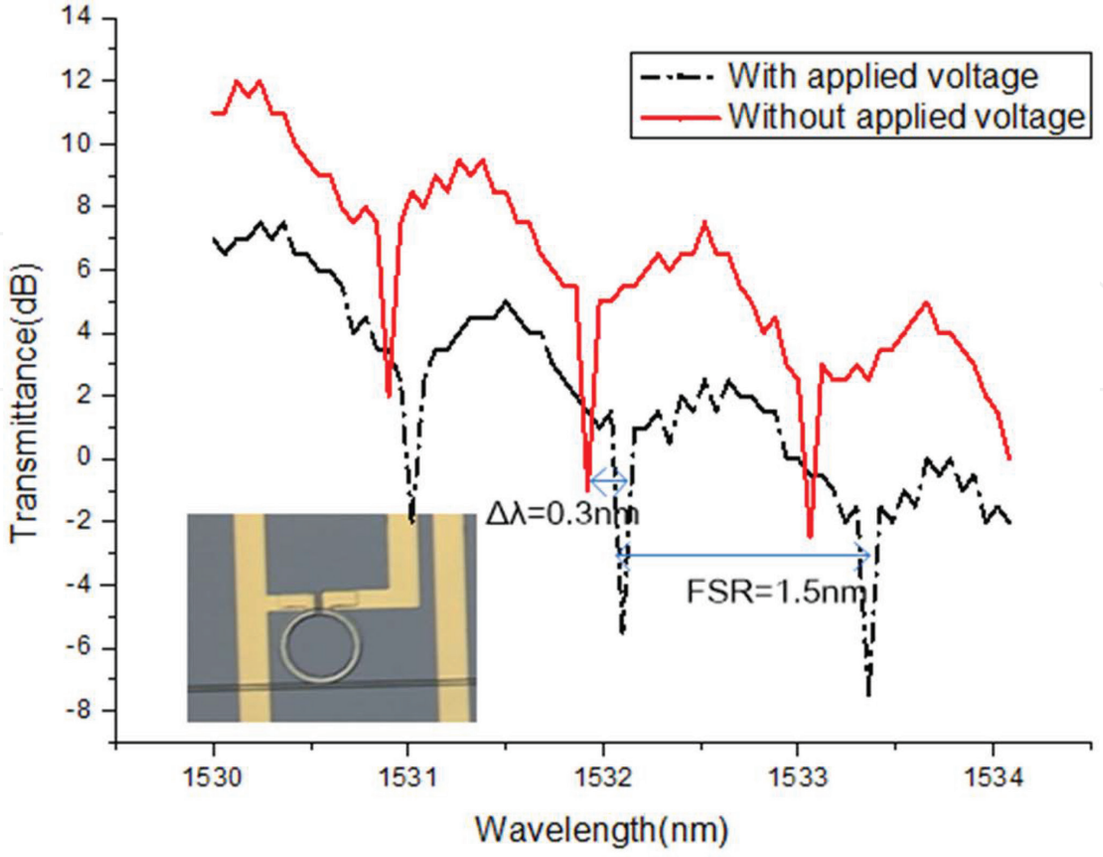

Figure 7. Wavelength shift of transmission spectrum in coupled-ring-resonator.

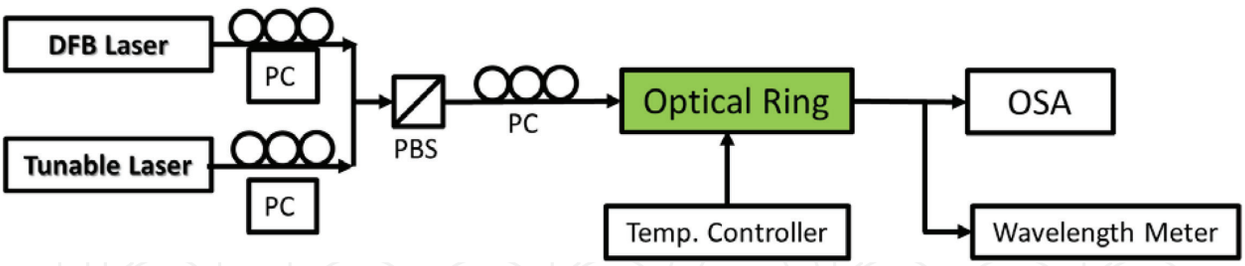

Figure 8. Optical micro-ring measurement platform.

With a linear raster coupler, the input light is coupled to this raster coupler for propagation, which is a linear raster structure limitation. Light requires longer focal length when traveling. If the focal length is not enough, easily lead to the scattering of light lead to energy loss. It causes the grating coupler coupling efficiency to drop.

In this study, the curvature-type grating structure is used for the measurement as shown in **Figure 10**. It can reduce the focusing length a lot. It is not loss of coupling efficiency.

Under the same coupling gap, the energy coupling coefficient and energy loss are relatively larger and larger in radius. The main reason is the large radius of the micro-ring coupling longer. Its energy coupling distance is longer. Therefore, a larger energy coupling coefficient

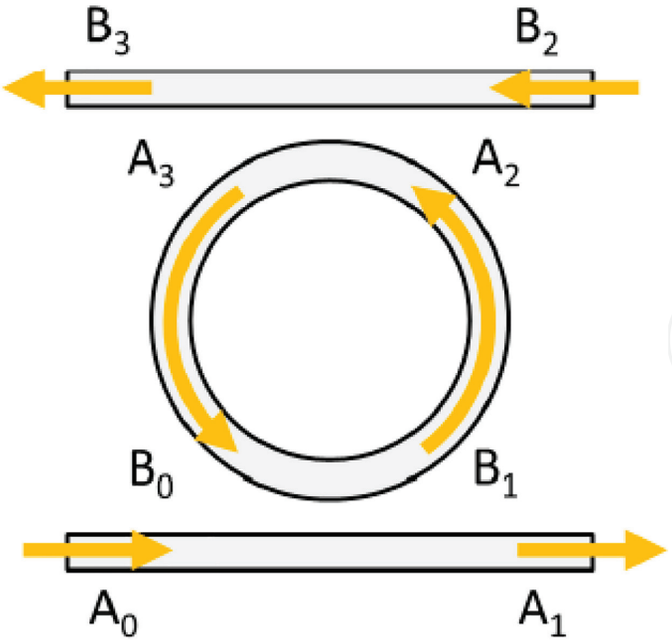

Figure 9. In add/drop condition.

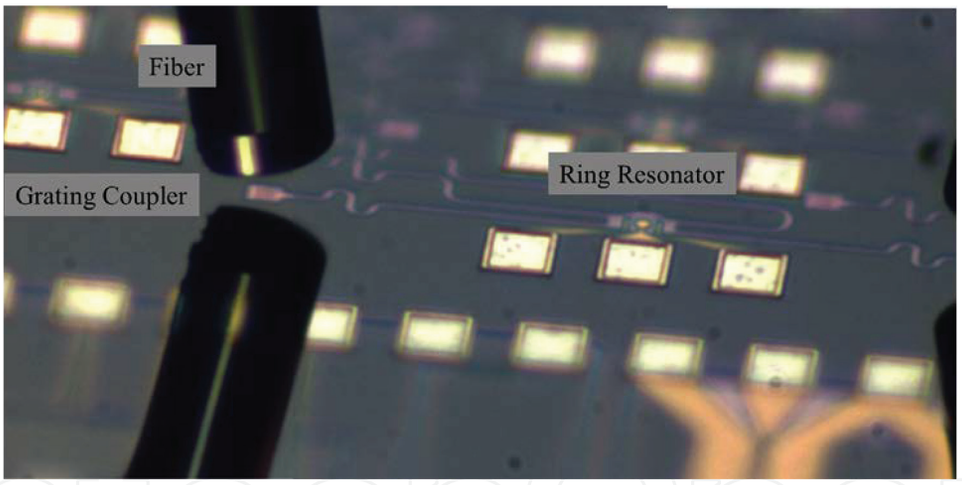

Figure 10. The vertical coupling system.

and coupling loss are generated. In addition, the total optical path of large radii in the ring resonator is larger than the small radius micro-rings. It produces extra spreading loss. Under the same coupling gap (200 μm) and radius 7.5 μm is shown in **Figure 11(a)**. Under the same coupling gap (200 μm) and radius 2.5 μm is shown in **Figure 11(b)**. Under the same coupling gap (200 μm) and radius 7.5 μm only drop is shown in **Figure 11(c)**.

It takes a drop of R2.5 Gap 200 at an approximate wavelength of 1546 nm. The dip curve with drop (with drop) and the dip curve with no drop (without drop) are shown in **Figure 12**.

It takes a drop of R7.5 Gap 200 at a wavelength of approximately 1555 nm. The dip curve with drop (with drop) and the dip curve with no drop (without drop) are shown in **Figure 13**. It is

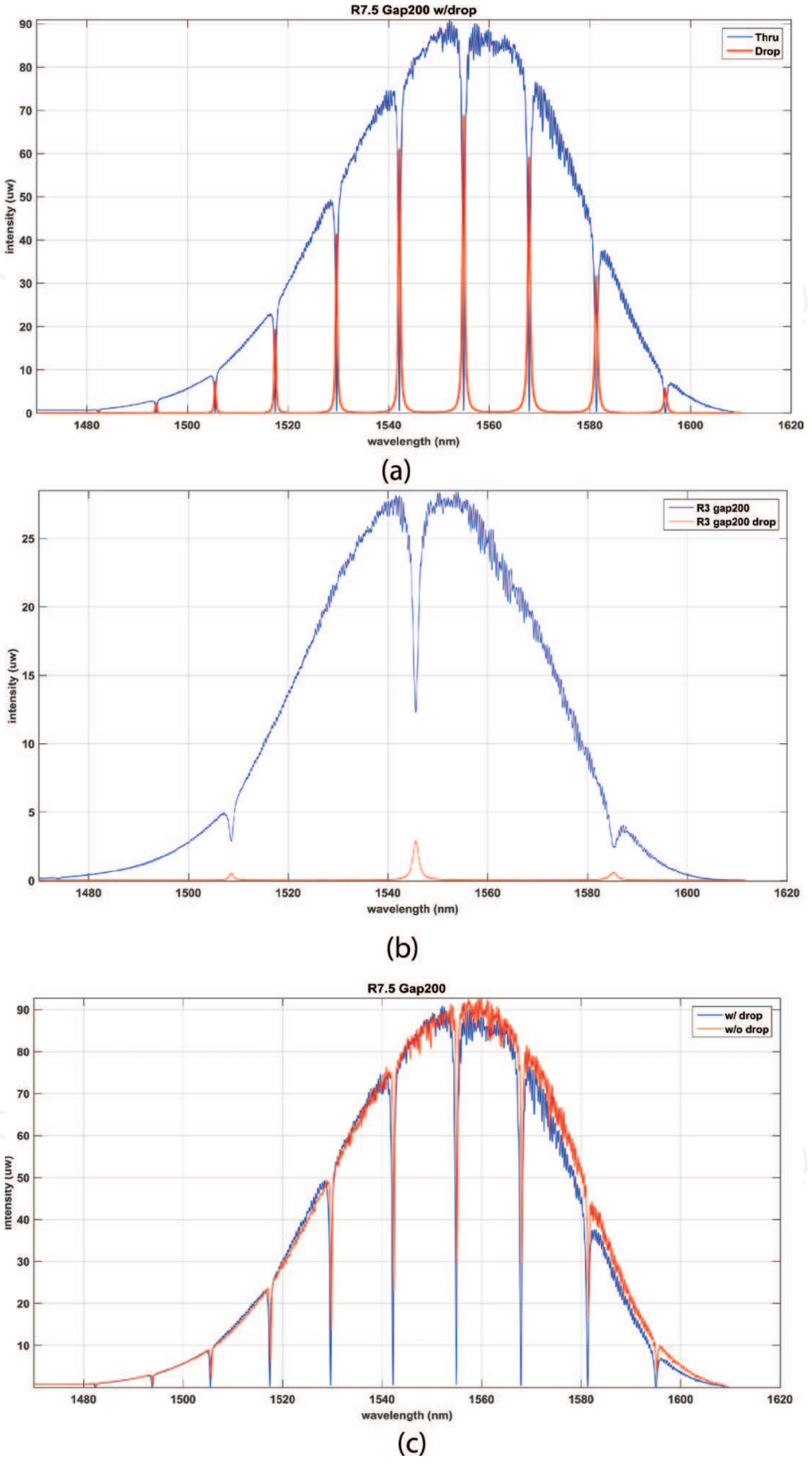

Figure 11. (a) Under the same coupling gap (200 μm) and radius 7.5 μm. (b). Under the same coupling gap (200 μm) and radius 2.5 μm. and (c). Under the same coupling gap (200 μm) and radius 7.5 μm only drop.

http://dx.doi.org/10.5772/intechopen.76800

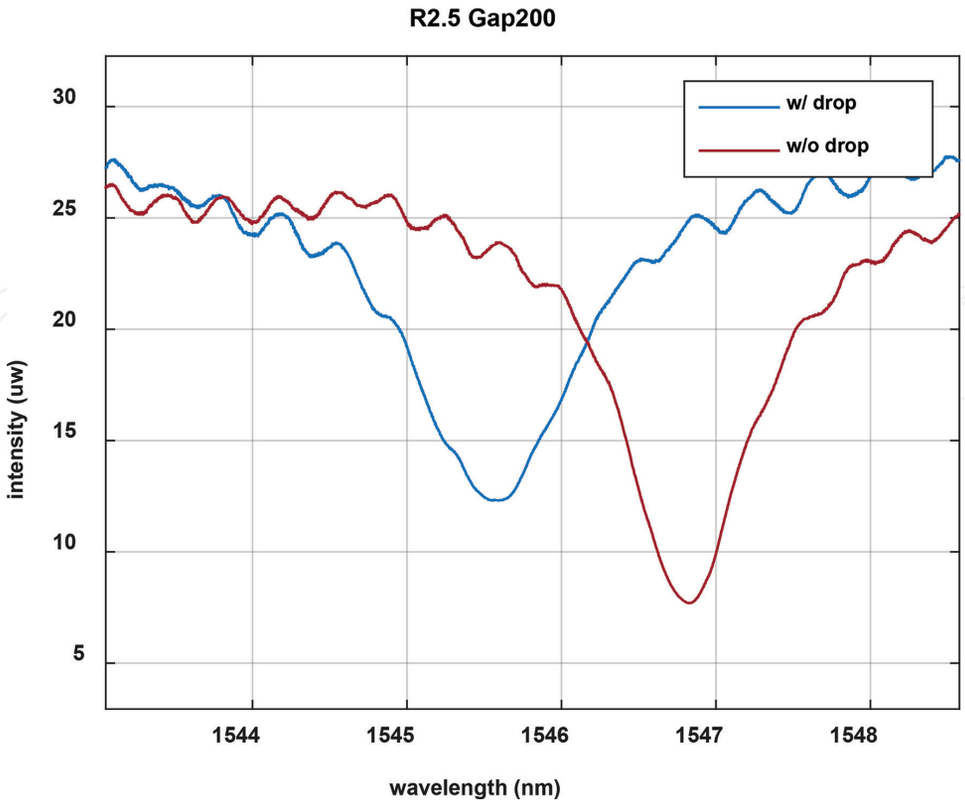

Figure 12. Take a drop of R2.5 gap 200 at an approximate wavelength of 1546 nm.

obviously very different. In the case of smaller micro-rings (R2.5 Gap 200), it presents a different drop wavelength. They differ by about 1 nm. In the case of large micro-rings (R7.5 Gap 200), it shows the same drop wavelength.

It adopts CMOS processing compatible processing methods. It has prepared a variety of types of grating coupler. Among them, it is in improving the coupling efficiency. It based on optimizing uniform grating structure parameters. It is reduce the reflection loss by covering the multilayer dielectric film. Use slot effect to increase the specific diffraction intensity. The non-uniform periodic structure is designed to realize the Gaussian field of diffraction field. Coupling efficiency continues to increase. It is 44% from conventional uniform grating couplers. It is 65% of the multilayer dielectric film grating structure. The coupling efficiency measurement of the non-uniform grating structure has reached 81.8%. In the vertical coupling by adding a DBR mirror. The second-order reflection at one end is canceled by the DBR reflected light interference. Vertical coupling was successfully achieved. In addition, the slope of the blazed grating is replaced by a step-change step structure. The analogy shows that the number of steps in a raster is 5. It could approximate the "shine" function.

The biggest advantage of a grating coupler lies in its testing and integration aspects. It compared to the face coupler. Grating couplers do not need to be polished. No strict space restrictions. Alignment tolerance, processing requirements are relatively simple. It greatly increased the flexibility of system design. It is more suitable for large-scale integration. It is in the

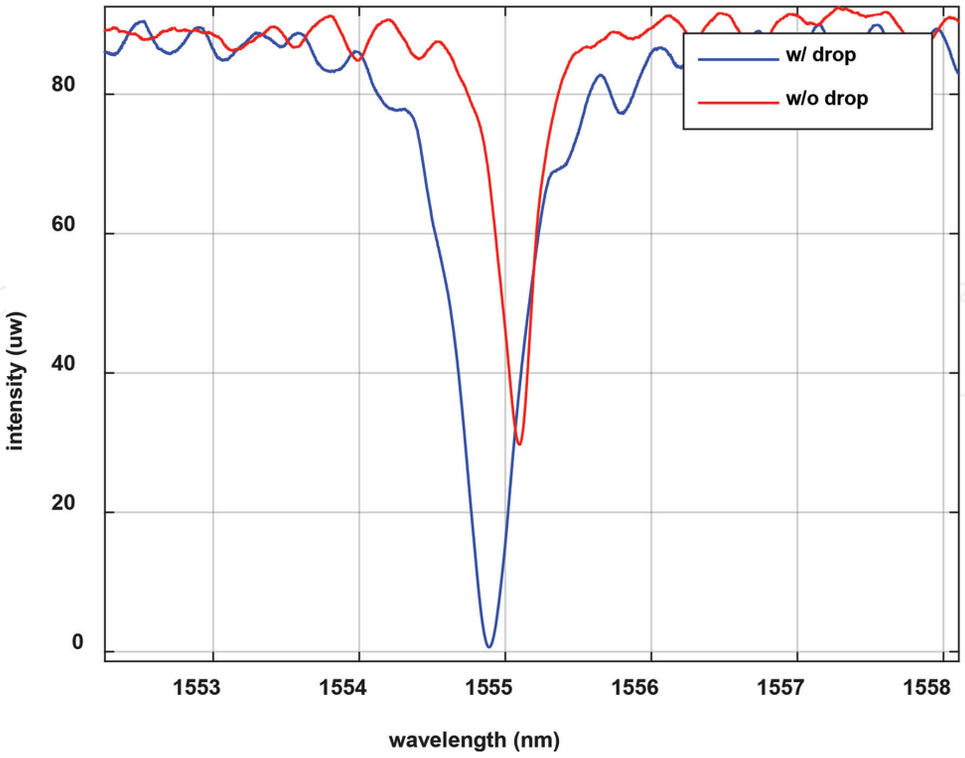

Figure 13. Take a drop of R7.5 gap 200 at a wavelength of approximately 1555 nm.

reported hybrid optoelectronic integration studies. Grating coupler compared with other coupling methods. Performance improvement is significant. The deepening of research work and the continuous development is preparation technology. The coupling efficiency of the grating coupler, working wavelength, polarization mode and other characteristics will continue to improve. It can be expected that grating couplers with high efficiency, large bandwidth and vertical coupling will rapidly develop and mature in the practical direction. A key element is in silicon-based photonics integration.

6. Author biography

Dr. Jian-Chiun Liou received a Ph.D. degree from the Institute of Nanoengineering and Microsystems, National Tsing Hua University, Hsinchu, Taiwan, in 2009. He joined the Printing Technology Development and Manufacturing Section of the Optoelectronics and Systems Laboratories at the Industrial Technology Research Institute (ITRI), Hsinchu, in 1999, where he focused on the ink-jet printing system. Since 2005, he has been a Project Leader working on a new MEMS architecture design and display application in the Electronics and Optoelectronics Research Laboratories, ITRI. In August 2014, he joined the faculty of the National Kaohsiung University of Applied Sciences (KUAS). In August 2017, he has joined the School of Biomedical Engineering, Taipei Medical University (TMU), Taipei 11,031, Taiwan. Currently, he is a Professor of School of Biomedical Engineering at the TMU. His research interests are in the fields of Optoelectronics, ASIC design, bio-chip technology, optical MEMS technology, integration of ink-jet printhead processes, and display technology. He is a holder of 71 patents on ink-jet printheads, MOEMS, MEMS, and has written more than 28 SCI Journal papers and

38 conference technical papers on MEMS, optical-N/MEMS, and display-related and micro−/nano-fluidics-related fields. He has also co-chaired many conference technical sessions and has been an invited speaker in many related events. In addition, he has performed the following tasks: Advance project leader (ITRI), SCI Journal paper reviewer (PIER, JEMWA, MEE), and Research fellow (NTHU). To add, Dr. Liou was the recipient of the following honors: ITRI/OES Research Achievement Award (2004), ITRI Research Paper Publication Award (2004), ITRI/EOL Research Achievement Award (Individual person Award, 2005), ITRI/EOL Outstanding Advanced Research Silver Award (2005), ITRI/EOL Research Achievement Award (2006), ITRI/EOL Patents Reviewer (2007), Outstanding Research Award (2007), ITRI/EOL Patents Reviewer(2008), Outstanding Research Award (2010), ITRI/EOL Patents Reviewer (2009), ITRI/EOL Outstanding Research Award (2010), International R&D 100 Awards (2010), 1st International Contest of Applications in Nano-Micro Technology Award (2010)—OPTO- MEMS Device Application, ITRI Paper Awards (2012), ITRI/EOL Outstanding Advanced Research Silver Award (2013), International Inventor Prize (2014), Nation Academic Award (2014). 2014 Invention Lifetime Achievement Award. 2015 "Design and fabrication of Monolithic CMOS/MEMS system with HV-ESD Clamp protected inkjet printhead." 2015 International Contest Application Contest in Nano-Micro Technology (Alaska, USA) "iCAN'15 7th Special Prize" 2015 International Contest of Application in Nano-Micro Technology (iCAN'15). Who's Who in the World® 2016 (33rd Edition). In 2016, "The 16th Wang Golden silicon semiconductor design and application contest winners": An ASIC designed to spray liquid medical wisdom DNA gene sequencing system. 2016 Third Prize Award and Best Supervisors: Jian-Chiun Liou, 2016 iCAN'16 France 2016 International Contest of Application in Nano-Micro Technology (iCAN'16 ESIEE Paris, July 7th, 2016): The Glove. 2017 "iCAN'17 Third Prize Award, and Education Star Award 2017 International Contest of Application in Nano-Micro Technology (iCAN'17 BEIJING): Cloud Health Care (CHC). 2017 Teaching Excellence Teacher Award. August 2017 Transferred to Taipei Medical University for medical electronics-related fields in-depth study. He is a member of the IEEE and a reviewer for more than 20 international journals including the Applied Physics Letters, JMEMS, Microfluidics and nano-fluidics, and micro-devices. He has also been a consultant to three Taiwanese companies.

Author details

Jian-Chiun Liou

Address all correspondence to: jcliou@tmu.edu.tw

School of Biomedical Engineering, Taipei Medical University, Taipei, Taiwan

References

[1] Kaalund CJ, Peng G. Pole-zero diagram approach to the design of ring resonator-based filters for photonic applications. Journal of Lightwave Technology. 2004;**22**(6):1548-1558

[2] Wang Z, ChenW, Chen YJ. Unit cell design of crossbar switch matrix using micro-ring resonators. ECOC 04, page we 3.7.2

[3] Chu ST, Little BE, Pan WG, Kaneko T, Kokubun Y. Cascaded microring resonators for crosstalk reduction and spectrum cleanup in adddrop filters. IEEE Photonics Technology Letters. 1999;**11**:1423-1425

[4] Chu ST, Little BE, Pan WG, Kaneko T, Sato S, Kokubun Y. An eight-channel add-drop filter using vertically coupled microring resonators over a cross grid. IEEE Photonics Technology Letters. 1999;**11**:691-693

[5] Ma X, Kuo GS. Optical switching technology comparison: Optical MEMS vs. other technologies. IEEE Communications Magazine. November, 2003;**41**(11):s16-s23

[6] Dey D. Towards an All-Optical WDM Slotted-Ring MAN with Support for Optical Multicasting. University of Twente. 19 Jun 2003. ISBNs:90-365-1930-6

[7] Smit MK, van Dam C. PHASAR-based WDM-devices: Principles, design and applications. IEEE Journal of Selected Topics in Quantum Electronics. 1996;**2**(2):236-250

[8] Smit MK. Arrayed Waveguide Devices: Where Do they Go from Here? Proc. Europ. Conf. Integrated Optics. France: Grenoble; 2005

[9] Fukazawa T, Ohno F, Baba T. Very compact arrayed-waveguide-grating demultiplexers using Si photonic wire waveguides. Japanese Journal of Applied Physics. 2004;**43**(5B):673-675

[10] Shibata T, Okuno M, Goh T, Watanabe T, Yasu M, Itoh M, Ishii M, Hibino Y, Sugita A, Himeno A. Silica-based waveguide-type 16 x 16 optical switch module incorporating driving circuits. IEEE Photonics Technology Letters. 2003;**15**(9):1300-1302

[11] Suzuki K, Mizuno T, Oguma M, Shibata T, Takahashi H, Hibino Y, Himeno A. Low loss fully reconfigurable wavelength-selective optical 1 x n switch based on transversal filter configuration using silica-based planar lightwave circuit. IEEE Photonics Technology Letters. 2004;**16**(6):1480-1482

[12] Kasahara R, Yanagisawa M, Goh T, Sugita A, Himeno A, Yasu M, Matsui S. New structure of silica based planar lightwave circuits for lowpower thermooptic switch and its application to 8 x 8 optical matrix switch. Journal of Lightwave Technology. 2002;**20**(6):993-1000

[13] Goh T, Yasu M, Hattori K, Himeno A, Okuno M, Ohmori Y. Low loss and high extinction ratio strictly nonblocking 16 x 16 thermooptic matrix switch on 6-in wafer using silica-based planar lightwave circuit technology. Journal of Lightwave Technology. 2001;**19**(3):371-379

[14] Mazumder MM, Hill SC, Chowdhury DQ, Chang RK. Dispersive optical bistability in a dielectric sphere. Journal of the Optical Society of America-B. 1995;**12**(2):297-310

[15] Haavisto J, Pajer GA. Resonance effects in low-loss ring waveguides. Optics Letters. 1980;**5**(12):510-512

[16] Weiershausen W, Zengerle R. Photonic highway switches based on ring resonators used as frequency-selective components. Applied Optics. 1996;**35**:5967-5978

[17] Little BE, Chu ST, Pan W, Kokubun Y. Microring resonator arrays for VLSI photonics. IEEE Photonics Technology Letters. 2000;**12**:323-325

[18] Suzuki S, Shuto K, Hibino Y. Integrated-optic ring resonators with two stacked layers of silica waveguide on Si. IEEE Xplore: IEEE Photonics Technology Letters. 1992;**4**(11): 1256-1258

[19] Madsen CK, Zhao JH. Optical Filter Design and Analysis. Wiley; 9 Oct 2001. (Print) ISBN: 9780471183730, (Online) ISBN: 9780471213758

[20] Driessen A, Geuzebroek DH, Hoekstra HJWM, Kelderman H, Klein EJ, Klunder DJW, Roeloffzen CGH, Tan FS, Krioukov E, Otto C, Gersen H, van Hulst NF, Kuipers L. Microresonators as building blocks for VLSI photonics. AIP Conference Proceedings. 2003;**709**:1-18

[21] Chao FL, Wang WS. Analysis of temperature profiles of thermo-optic waveguides. Fiber and Integrated Optics. 1994;**13**:397-406

[22] Wang WK, Lee HJ, Anthony PJ. Planar silica-glass optical waveguides with thermally induced lateral mode confinement. IEEE Journal of Lightwave Technology. 1996;**14**:429-436

[23] Hryniewicz JV. Higher order filter response in coupled microring resonators. IEEE Photonics Technology Letters. 2000;**12**:320-322

[24] Orta R, Savi P, Tascone R, Trinchero D. Synthesis of multiplering- resonator filters for optical systems. IEEE Photonics Technology Letters. 1995;**7**:1447-1449

[25] Rabus DG, Hamacher M, Heidrich H. Resonance frequency tuning of a double ring resonator in GaInAsP/InP: Experiment and simulation. Japanese Journal of Applied Physics. 2002;**41**(2B):1186-1189

[26] Madsen CK, Zhao JH. A general planar waveguide autoregressive optical filter. Journal of Lightwave Technology. 1996;**14**:437-447

[27] Little BE, Chu ST, Absil PP, Hryniewicz JV, Johnson FG, Seiferth F, Gill D, Van V, King O, Trakalo M. Very high-order microring resonator filters for WDM applications. IEEE Photonics Technology Letters. 2004;**16**(10):2263-2265

[28] Kim G-D, Lee S-S. Photonic microwave channel selective filter incorporating a thermooptic switch based on tunable ring resonators. IEEE Photonics Technology Letters. July1, 2007;**19**(13):1008-1010

[29] Tewary A, Digonnet MJF, Sung J-Y, Shin JH, Brongersma ML. Silicon-nanocrystal-coated silica microsphere thermooptical switch. IEEE Journal of Selected Topics in Quantum Electronics. November/December, 2006;**12**(6):1476-1479

[30] Tapalian HC, Laine J-P, Lane PA. Thermooptical switches using coated microsphere resonators. IEEE Photonics Technology Letters. August, 2002;**14**(8):1118-1120

[31] Il'chenko VS, Gorodetskii ML. Thermal nonlinear effects in optical whispering gallery microresonators. Laser Physics. 1992;**2**:1004-1009

[32] Davis MK, Digonnet MJF, Pantell RH. Thermal effects in doped fibers. Journal of Lightwave Technology. June, 1998;**16**(6):1013-1023

[33] Ng HY, Wang MR, Li D, Wang X, Martinez J, Panepucci RR, Pathak K. 1×4 wavelength reconfigurable photonic switch using thermally tuned microring resonators fabricated on silicon substrate. IEEE Photonics Technology Letters. May 1, 2007;**19**(9):704-706

[34] Lienhard JH IV, Lienhard JH V. A Heat Transfer Textbook. Cambridge Massachusetts: Phlogistron Press; 2003

[35] Ozisik MN. Boundary Value Problems of Heat Conduction. NewYork: Dover; 1989

[36] Worhoff K, Hilderink LTH, Driessen A, Lambeck PV. Silicon oxynitride—A versatile material for integrated optics applications. Journal of The Electrochemical Society. 2002;**149**(8):F85-F91